Supporting Information

Hanker et al. 10.1073/pnas.1303204110

SI Materials and Methods

Transgenic Mice. All transgenic mice were maintained on a high-fat diet (5LJ5; LabDiet). Mice were administered 2 mg/mL doxycycline (DOX) in 5% sucrose water as published previously (1) or 5% sucrose water alone (vehicle control) beginning at 4 wk of age. Fresh DOX water was replaced twice weekly. Tumor formation was monitored twice weekly by palpation. Tumor volume in cubic millimeters was calculated by the formula: volume = width^2 × length/2. Tumor-free survival was analyzed using the Kaplan–Meier method. Mice were killed when total tumor volume reached 1,500–2,000 mm^3 or when animals showed signs of distress or tumor hemorrhage. All genotypes were confirmed by PCR of mouse tail DNA at time of killing.

In Vivo Bioluminescent Imaging. Luciferase gene expression in live mice was monitored using the Xenogen IVIS 200 imaging system. Mice were anesthetized with isoflurane and administered 2 mg VivoGlo Luciferin (Promega) dissolved in PBS and administered i.p. 15–20 min before imaging. Images were captured using Living Image 4.0 software. Imaging was performed at the Center for Small Animal Imaging, Vanderbilt University Institute of Imaging Science.

Histological Analysis, Immunohistochemistry, and Immunofluorescence. Whole mammary glands (no. 4 inguinal) were fixed in 10% neutral-buffered formalin (NBF), mounted on glass slides, and stained with hematoxylin, as described previously (2). Mammary glands, tumors, and lungs were fixed in 10% NBF and embedded in paraffin. Sections (5 μm) were stained with hematoxylin and eosin (H&E), or used for immunohistochemistry (IHC) of Cytokeratin 14 (Thermo Scientific; RB-9020; 1:1,000), Cytokeratin 18 (Abcam; ab32118; 1:100), Snail/Slug (Abcam; ab85936), p63 (Sigma; P3737; 1:800), Vimentin (Epitomics; 2707–1), Ki67 (Zymed Invitrogen), phospho-AKT^{S473} (Cell Signaling Technologies; 4060; 1:10), or terminal deoxynucleotidyl transferase-mediated dUTP nick end labeling (TUNEL) analysis (ApopTag In Situ Apoptosis Detection kit; EMD Millipore). An expert breast pathologist (M. G.K.) blinded to the mouse genotypes/treatments scored the sections and diagnosed the histopathology of each tumor. The intensity of cytoplasmic p-AKT staining was graded using a score of 0–300 as described (3). Images were obtained using Olympus DP2 software on an Olympus light microscope.

For tissue immunofluorescence (IF), following antigen retrieval with pepsin, 5-μm sections were stained with either trastuzumab (21 μg/mL) followed by Alexa Fluor 488 antihuman IgG (Invitrogen; 1:100) or HA (Cell Signaling; 3724; 1:25) followed by Alexa Fluor 594 anti-rabbit IgG (Invitrogen; 1:500). Images were captured from an upright microscope (Axioplan 2; Carl Zeiss) using MetaMorph software (MDS Analytical Technologies). Co-localization analysis of IF signals was performed using MetaMorph software. Briefly, background (median filter of 32 × 32 pixels) was subtracted from the original image and a threshold of 116 was set for both channels. Percent overlap for each channel (green and red) was calculated using the Measure Colocalization application.

Western Blot Analysis. Snap-frozen mammary glands or tumors were homogenized and lysed in buffer containing 50 mM Tris·HCl pH 8.0, 150 mM NaCl, 2 mM EDTA pH 8.0, 10 mM NaF, 20% glycerol, 1% Nonidet P-40, plus protease and phosphatase inhibitors. Lysates were cleared by centrifugation at >20,000 × g for 10 min. Protein concentration was determined using the bicinchoninic acid (BCA) assay (Pierce). Lysates were resolved on SDS/PAGE gels and transferred to nitrocellulose membranes. The following antibodies were used: phospho-human epidermal growth factor receptor 2 (HER2) Y1248 (1:500), phospho-HER3 Y1289 (1:1,000), HA (1:1,000), phospho-AKT T308 (1:500), phospho-AKT S473 (1:500), AKT (1:1,000), phospho-PRAS40 T246 (1:1,000), PRAS40 (1:1,000), phospho-S6 S240/S244 (1:1,000), S6 (1:1,000), phospo-ERK1/2 T202/Y204 (1:1,000), ERK1/2 (1:1,000), E-cadherin (1:1,000), N-cadherin (1:500), and Vimentin (1:1,000) (all Cell Signaling), HER2 (Neomarkers; 1:1,000), HER3 (Santa Cruz; 1:1,000), and β-actin (Sigma; 1:5,000).

Microarray Analysis. RNA was harvested from six *HER2* tumors (3 *HER2* + DOX and 3 *HER2* – DOX), six *phosphatidylinositol-4,5-bisphosphate 3-kinase, catalytic subunit alpha* (*PIK3CA*) tumors, and seven *HER2*$^+$*PIK3CA* tumors using the RNeasy Mini kit (Qiagen) according to the manufacturer's instructions. Appropriate HER2 and HA-PI3K expression was confirmed in all tumors by immunofluorescence and Western blot analysis. Total RNA was hybridized to custom Agilent 4 × 180 K mouse microarrays as previously described (4). The microarray data were uploaded to the University of North Carolina Microarray Database (UMD; https://genome.unc.edu/pubsup/breastGEO/clinicalData.shtml) and to the Gene Expression Omnibus (GEO) under accession no. GSE41118. Microarray samples were combined into a single dataset with other murine models of mammary carcinoma [GSE3165 (4) and GSE27101 (5)] using normalization methods as previously described (6). Gene expression signatures were derived using an unpaired, two-class ("tumors of interest" versus "all other tumors") significance analysis of microarray (SAM) analysis (7), with genes having a false discovery rate (FDR) of 0% being considered statistically different. The gene expression signature value for each tumor sample was determined by subtracting the average of down-regulated genes from the average of up-regulated genes. Tumor differentiation scores were calculated as previously described (8).

For clustering analysis, the data were first filtered for only those probesets that matched to a unique Entrez gene identification and with a coefficient of variation greater than 50% across all samples (6,804 unique genes). The data were then analyzed by ANOVA using a three-class comparison. Multiple comparisons were corrected for by adjusting the P values using the Benjamini and Hochberg method (9). An FDR cutoff of 0.05 resulted in a dataset of 81 significantly altered genes. These data were then used for hierarchical clustering in R.

Gene Set Analysis. Gene set analysis (GSA), a variation on Gene Set Enrichment Analysis (GSEA) (10), was performed in R (www.r-project.org) using the package GSA. First, the mouse gene arrays were mapped to the human orthologs. Three classes (*PIK3CA*, *HER2*, and *HER2*$^+$*PIK3CA*) were analyzed by GSA using the "multiclass" algorithm and the "maxmean" option. Gene sets from the C2 curated Molecular Signatures Database (10) version 3.0, with a minimum size of five genes, were considered for GSA. Enriched gene sets were chosen at a FDR of 0.2.

Tumor Dissociation and Mammosphere Assay. Mammary tumors were harvested, minced, and homogenized in DMEM/F12 medium containing 5% FBS using gentleMACS C tubes (Miltenyi Biotec). Collagenase/hyaluronidase (1×; Stem Cell Technologies) and 40 μg/mL DNaseI (Stem Cell Technologies) were added; homogenized tumors were incubated at 37 °C for 0.5–2 h. Dissociated tumor cells were then passed through 70- and 35-μm

filters. An equal volume of Ficoll-Paque PLUS (GE Healthcare) was added and dissociated tumors were centrifuged at high speed with breaks turned off. Cells found at the gradient were isolated and counted in Trypan blue solution. For the mammosphere assay, 10^4 viable cells were plated per well of six-well ultra-low attachment plates (Costar) in triplicate and maintained in serum-free DMEM/F12 containing 1× B27, 20 ng/mL EGF, 20 ng/mL bFGF, 4 μg/mL heparin ± 1 μg/mL DOX. Where indicated, trastuzumab (20 μg/mL) or BKM120 (1 μM) were added the day after plating. Media containing fresh drug and DOX was replenished every 3 d and mammospheres were quantified after 12–13 d using the GelCount mammalian cell colony counter (Oxford Optronix). For bioluminescent imaging, 150 ng/mL luciferin was added to the media and plates were imaged using the Xenogen IVIS 200 imaging system.

Tail Vein Injection Metastasis Assay. Mammary tumors were homogenized, dissociated, and filtered as above. Tumor epithelial cells were isolated using the EasySep Mouse Epithelial Cell Enrichment kit (Stem Cell Technologies) according to the manufacturer's instructions and resuspended in serum-free DMEM. A total of 10^5 cells in 100 μL media were injected into the tail vein of 7- to 8-wk-old nude mice using a 27-gauge needle. Nude mice were maintained on 2 mg/mL DOX drinking water. After 32 d, lungs were harvested, fixed in 10% NBF, and embedded in paraffin. Serial sections (5 μm each) were taken every 50 μm and stained with H&E. The number of lung metastases was scored for each H&E section. The polygon tool in LP2 software was used to measure the area of each lung metastasis on the fifth H&E section for each mouse.

Tumor Transplants and Drug Treatments. *HER2* or *HER2*+*PIK3CA* mammary tumors were harvested, homogenized as above in DMEM + antibiotics/antimycotics, and mixed 1:1 with growth factor-reduced Matrigel (BD Biosciences); 200–300 μL of homogenized tumor/Matrigel was injected into the inguinal mammary fat pads of 5- to 7-wk-old athymic female nude mice (Harlan) using a 25-gauge needle. Mice were maintained on 2 mg/mL DOX drinking water. Trastuzumab (30 mg/kg in sterile PBS; Vanderbilt University Pharmacy) and pertuzumab (30 mg/kg in sterile PBS; Vanderbilt University Pharmacy) were administered i.p. twice weekly. BKM120 (30 mg/kg; Novartis) and lapatinib (100 mg/kg; LC Laboratories) were administered daily by oral gavage in 0.5% hydroxypropylmethylcellulose, 0.1% Tween-80. Tumors were measured with calipers two times per week and tumor volume in cubic millimeters was calculated using the formula volume = width^2 × length/2. Mice were killed and tumors were harvested after 2–4 wk of treatment, 1 h after the last dose of BKM120 or lapatinib and 24 h after receiving trastuzumab or pertuzumab.

1. Gunther EJ, et al. (2002) A novel doxycycline-inducible system for the transgenic analysis of mammary gland biology. *FASEB J* 16(3):283–292.
2. Muraoka RS, et al. (2002) ErbB2/Neu-induced, cyclin D1-dependent transformation is accelerated in p27-haploinsufficient mammary epithelial cells but impaired in p27-null cells. *Mol Cell Biol* 22(7):2204–2219.
3. Garrett JT, et al. (2011) Transcriptional and posttranslational up-regulation of HER3 (ErbB3) compensates for inhibition of the HER2 tyrosine kinase. *Proc Natl Acad Sci USA* 108(12):5021–5026.
4. Herschkowitz JI, et al. (2007) Identification of conserved gene expression features between murine mammary carcinoma models and human breast tumors. *Genome Biol* 8(5):R76.
5. Herschkowitz JI, et al. (2012) Comparative oncogenomics identifies breast tumors enriched in functional tumor-initiating cells. *Proc Natl Acad Sci USA* 109(8):2778–2783.
6. Roberts PJ, et al. (2012) Combined PI3K/mTOR and MEK inhibition provides broad antitumor activity in faithful murine cancer models. *Clin Cancer Res* 18(19):5290–5303.
7. Tusher VG, Tibshirani R, Chu G (2001) Significance analysis of microarrays applied to the ionizing radiation response. *Proc Natl Acad Sci USA* 98(9):5116–5121.
8. Prat A, et al. (2010) Phenotypic and molecular characterization of the claudin-low intrinsic subtype of breast cancer. *Breast Cancer Res* 12(5):R68.
9. Benjamini Y, Hochberg Y (1995) Controlling the false discovery rate: A practical and powerful approach to multiple testing. *J R Stat Soc, B* 57(1):289–300.
10. Subramanian A, et al. (2005) Gene set enrichment analysis: a knowledge-based approach for interpreting genome-wide expression profiles. *Proc Natl Acad Sci USA* 102(43):15545–15550.

Fig. S1. DOX induction of luciferase expression in mammary glands and tumors. (*A*) The *MMTV-HER2* transgene allows mammary-specific expression of human HER2. In the *MMTV-rtTA* transgene, the reverse tetracycline-dependent transactivator (rtTA) is under the control of the MMTV promoter. In the presence of DOX, rtTA binds to the tet operator (TetOp) and induces transcription of the third transgene, containing *PIK3CA^{H1047R}*, an internal ribosomal entry site (IRES) and the firefly luciferase gene. In the absence of DOX, rtTA is inactive, and mutant PI3K and luciferase are not expressed. Mice were bred to express all three transgenes (*HER2^{+}PIK3CA* mice). (*B*) Female mice were administered 2 mg/mL DOX or vehicle in their drinking water beginning at 4 wk of age. Following 1 wk of DOX, mice were injected with 2 mg luciferin i.p. and bioluminescence was imaged using the Xenogen IVIS 200 Imaging system.

Fig. S2. Human HER2 and PI3K^{H1047R} dysregulate proliferation and mammary gland morphogenesis. (*A*) No. 4 inguinal mammary glands were harvested from 12-wk-old mice (8 wk ± DOX) of the indicated genotypes. Mice were administered DOX beginning at 4 wk of age. Whole mammary glands were fixed in 10% NBF, mounted on glass slides, and stained with hematoxylin or paraffin-embedded and stained with H&E, pAKT^{S473}, and Ki67 or subjected to TUNEL analysis. [Scale bars, second row (from top), 500 μm; third row, 100 μm; fourth–sixth rows, 50 μm.] (*B–D*) Quantification of the staining in *A*. Error bars represent the average ± SD of three samples per group. (*B*) The percent of the section that stained positive for pAKT was scored. Percentage of Ki67 (*C*) and TUNEL (*D*) positive cells was scored by counting 300–400 cells in each section. *$P < 0.05$, **$P < 0.01$, ***$P < 0.001$, relative to WT; Student *t* test.

Fig. S3. *HER2*^{+}*PIK3CA* mice develop multiple fast-growing, hemorrhagic mammary tumors. (*A*) Number of mammary tumors per mouse was confirmed at killing and divided by age at killing. *$P < 0.05$, **$P < 0.01$, Tukey's multiple comparison test. (*B*) Total tumor volume was measured with calipers at time of killing and divided by age at killing. *$P < 0.05$, ***$P < 0.001$, Tukey's multiple comparison test. (*C*) The amount of time for a tumor to grow to 1,000 mm³ was calculated from the time of palpation. Tumors were measured with calipers twice weekly. *$P < 0.05$, Tukey's multiple comparison test. (*D–G*) H&E images of *HER2*^{+}*PIK3CA* primary tumors (*D*, *E*, and *G*) and lung metastasis (*F*) showing hemorrhagic areas or areas of high blood content. (*D*) Image showing large blood vessels adjacent to the tumor. (*E*) Image of a blood-filled tumor. (*F*) Image of a hemorrhagic lung metastasis. (*G*) Image of a hemorrhagic tumor showing hemosiderin-laden macrophages in the stroma. (*H–J*) H&E images of lung metastases from nude mice injected with cells from *HER2* (*H*), *PIK3CA* (*I*), or *HER2*^{+}*PIK3CA* (*J*) tumors. (Magnification: *D*, 4×; *E* and *F*, 10×; *G*, 20×; *H–J*, 10×; scale bar, 200 μm.)

Fig. S4. *PIK3CA* and *HER2*^{+}*PIK3CA* tumors are histologically heterogeneous and express luminal and basal markers. (*A*) Formalin-fixed, paraffin-embedded (FFPE) tumor sections from the indicated genotypes were stained with H&E or subjected to IHC with antibodies to cytokeratin 18 (luminal marker), cytokeratin 14 (myoepithelial/basal marker), or p63 (basal marker). (Scale bar, 200 μm.) (*B*) Histological phenotypes were quantified by an expert breast pathologist. ADC, adenocarcinoma; crib, cribriform. Only *HER2.rtTA.PIK3CA* + DOX tumors with confirmed expression of human HER2 and HA-PI3K were included in this analysis.

Fig. S5. Analysis of gene expression profiles for *HER2*, *PIK3CA*, and *HER2*^{+}*PIK3CA* tumors. RNA isolated from mouse mammary tumors of the indicated genotypes was hybridized to Agilent 4 × 180 k mouse microarrays. (*A*) Hierarchical clustering of gene expression profiles. An FDR cutoff of 0.05 was used, resulting in a dataset of 81 significantly altered genes. (*B*) Gene set analysis (GSA) of the mouse tumor gene expression microarrays was performed in R using the multiclass algorithm and the maxmean option. Gene sets from the C2 curated Molecular Signatures Database were considered for analysis. Enriched gene sets were chosen at a FDR of 0.2. Clustering was performed in R. ANOVA *P* values are shown in Table S1.

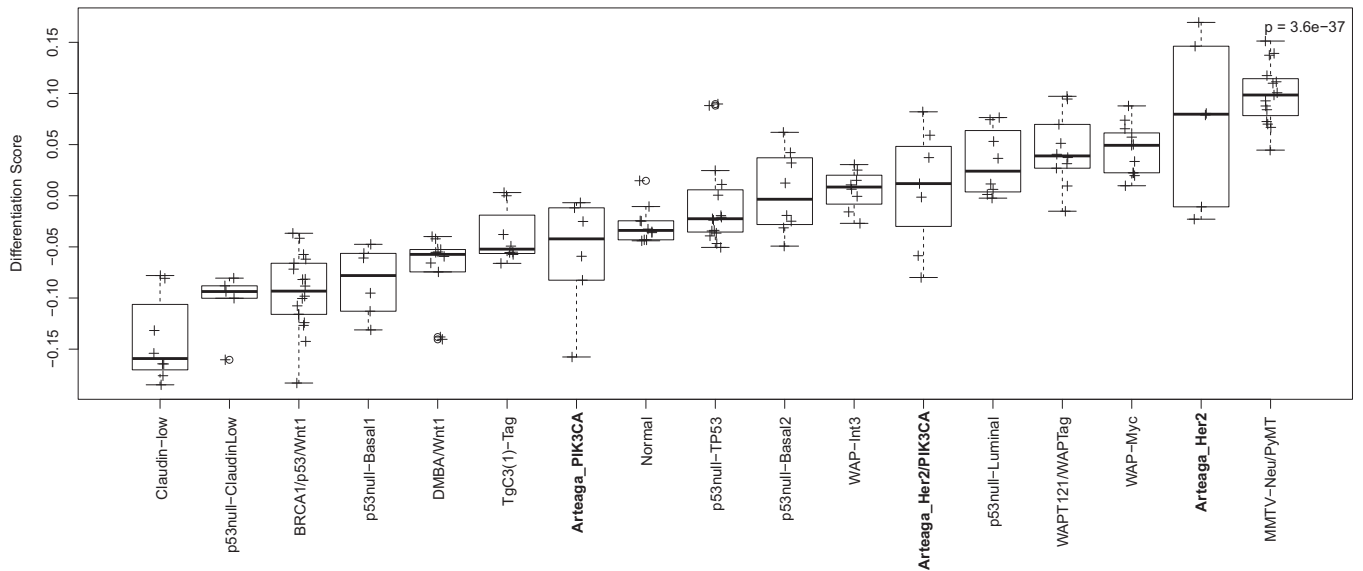**Herschkowitz GEMM Classes and Arteaga Her2 Differentiation Score**

Fig. S6. Tumor differentiation scores (D scores) were calculated and plotted against D scores from a series of transgenic mouse models of breast cancer as described in *SI Materials and Methods*. High D scores are indicative of gene expression profiles similar to mature luminal epithelial cells, whereas low D scores are more similar to mammary stem cells. The mouse models used in this study are highlighted in bold.
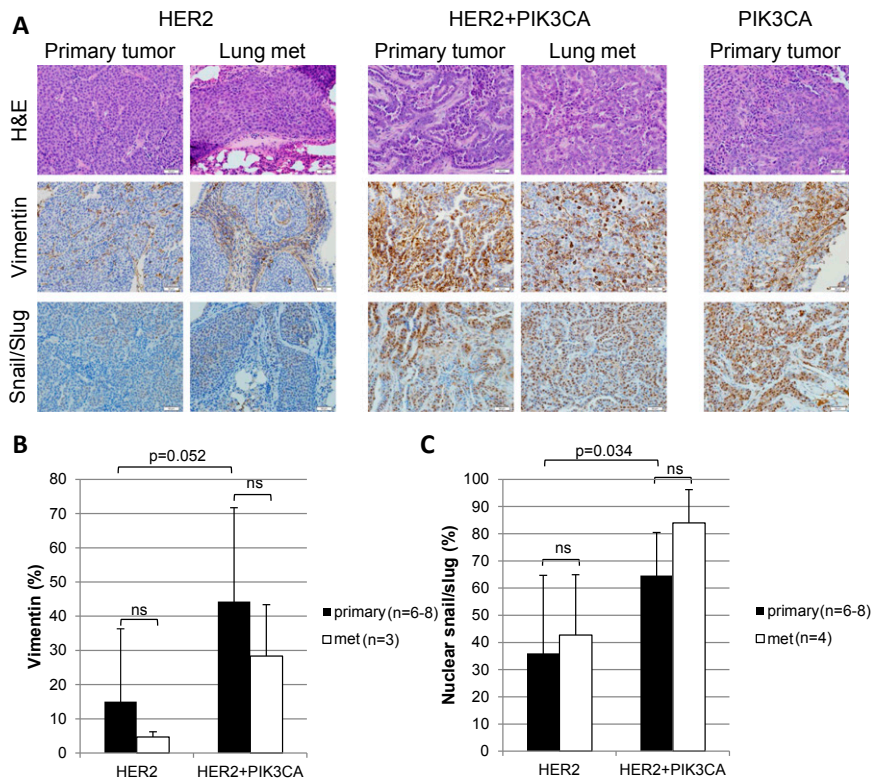
Fig. S7. Vimentin and Snail/Slug expression is elevated in *HER2⁺PIK3CA* tumors and lung metastases. (*A*) FFPE sections of matched primary mouse mammary tumors and lung metastases were stained with Vimentin and Snail/Slug by IHC as described in *SI Materials and Methods*. Matched *PIK3CA* lung metastases were insufficient for staining. (Scale bar, 50 μm.) (*B* and *C*) The percent of tumor cells that stained positive for Vimentin (*B*) or Snail/Slug (*C*) were quantified by an expert breast pathologist (M.G.K.). Error bars represent the average ± SD. *P* values were calculated using a Student *t* test.
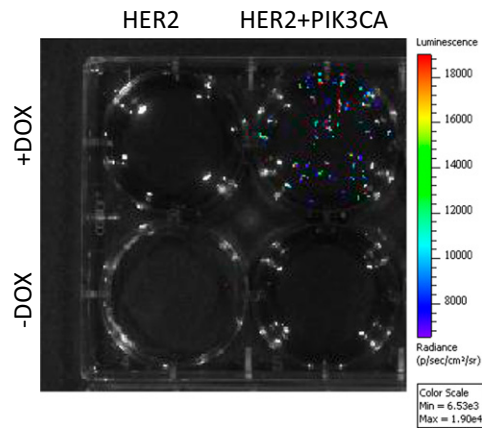
Fig. S8. Primary tumors of the indicated genotypes were dissociated and single cell suspensions were plated onto ultra-low attachment plates in mammo-sphere media ±1 µg/mL DOX. Luciferin was added to each well and bioluminescence was imaged 13 d after plating.
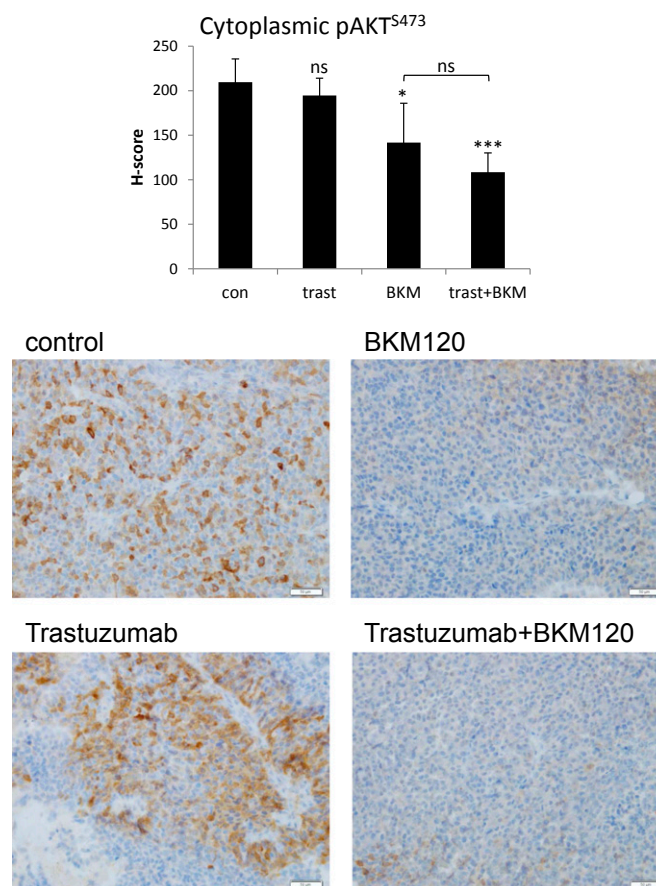
Fig. S9. BKM120 reduces p-AKT^{S473} IHC staining. Tumor tissue was collected from transplanted *HER2$^+$PIK3CA* tumors (n = 4–6 per group) at the end of treatment. FFPE tumor sections were stained with p-AKT^{S473} and quantified by a pathologist as described in *SI Materials and Methods*. Error bars represent the average ± SD. *$P < 0.05$, ***$P < 0.001$, relative to control; Student t test. Representative images are shown. (Scale bar, 50 µm.)

Table S1. Gene set analysis of *HER2*, *PIK3CA*, and *HER2+PIK3CA* tumors

Gene_set	Gene_set_name	Score	*P* value	FDR
886	**GUENTHER_GROWTH_SPHERICAL_VS_ADHERENT_DN**	0.6382	0	0
1649	ALONSO_METASTASIS_NEURAL_UP	1.1014	0	0
1841	ZHAN_V1_LATE_DIFFERENTIATION_GENES_UP	0.6816	0	0
2903	REACTOME_G_PROTEIN_BETA_GAMMA_SIGNALING	0.6231	0	0
253	TONKS_TARGETS_OF_RUNX1_RUNX1T1_FUSION_HSC_UP	0.3027	0.002	0.0239
1271	KANG_IMMORTALIZED_BY_TERT_UP	0.4843	0.002	0.0239
2483	**KEGG_PHOSPHATIDYLINOSITOL_SIGNALING_SYSTEM**	0.5144	0.002	0.0239
3028	REACTOME_PLC_BETA_MEDIATED_EVENTS	0.6778	0.002	0.0239
814	**LIEN_BREAST_CARCINOMA_METAPLASTIC**	0.9564	0.004	0.047
1251	LEI_MYB_TARGETS	1.3402	0.004	0.047
1647	**ALONSO_METASTASIS_EMT_UP**	0.5934	0.004	0.047
2510	KEGG_GAP_JUNCTION	0.4203	0.004	0.047
2673	BIOCARTA_IL5_PATHWAY	1.7121	0.004	0.047
207	GARGALOVIC_RESPONSE_TO_OXIDIZED_PHOSPHOLIPIDS_GREEN_UP	0.5655	0.006	0.0687
517	MAHADEVAN_IMATINIB_RESISTANCE_UP	0.8767	0.006	0.0687
1650	**ALONSO_METASTASIS_UP**	0.1852	0.006	0.0687
1964	STEIN_ESTROGEN_RESPONSE_NOT_VIA_ESRRA	0.7535	0.006	0.0687
2118	RODWELL_AGING_KIDNEY_NO_BLOOD_UP	0.5759	0.006	0.0687
2432	**KEGG_INOSITOL_PHOSPHATE_METABOLISM**	0.5163	0.006	0.0687
2999	REACTOME_OPIOID_SIGNALING	0.2793	0.006	0.0687
730	DIRMEIER_LMP1_RESPONSE_LATE_UP	0.4342	0.008	0.09
1399	KONDO_COLON_CANCER_HCP_WITH_H3K27ME1	0.5214	0.008	0.09
1529	SMID_BREAST_CANCER_RELAPSE_IN_PLEURA_UP	1.2029	0.008	0.09
1593	NAKAMURA_METASTASIS_MODEL_UP	0.4368	0.008	0.09
3078	REACTOME_SEMA4D_IN_SEMAPHORIN_SIGNALING	0.5211	0.008	0.09
586	GILMORE_CORE_NFKB_PATHWAY	1.0975	0.01	0.1105
1304	VERHAAK_AML_WITH_NPM1_MUTATED_DN	0.4133	0.01	0.1105
2124	KAAB_HEART_ATRIUM_VS_VENTRICLE_UP	0.3218	0.01	0.1105
2338	SESTO_RESPONSE_TO_UV_C7	0.345	0.01	0.1105
2716	BIOCARTA_EDG1_PATHWAY	0.5385	0.01	0.1105
440	CONCANNON_APOPTOSIS_BY_EPOXOMICIN_DN	0.3073	0.012	0.1294
1652	CROMER_TUMORIGENESIS_UP	0.8301	0.012	0.1294
2187	LIANG_SILENCED_BY_METHYLATION_UP	0.827	0.012	0.1294
2654	BIOCARTA_FREE_PATHWAY	0.7111	0.012	0.1294
2804	REACTOME_ADENYLATE_CYCLASE_ACTIVATING_PATHWAY	1.138	0.012	0.1294
2915	REACTOME_GLUCAGON_SIGNALING_IN_METABOLIC_REGULATION	0.5007	0.012	0.1294
3239	SIG_CHEMOTAXIS	0.2939	0.012	0.1294
749	SASAKI_TARGETS_OF_TP73_AND_TP63	1.2006	0.014	0.149
1544	ITO_PTTG1_TARGETS_DN	0.6912	0.014	0.149
3029	REACTOME_PLC_GAMMA1_SIGNALING	0.4466	0.014	0.149
3188	REACTOME_G_BETA_GAMMA_SIGNALING_THROUGH_PLC_BETA	0.5832	0.014	0.149
168	WIKMAN_ASBESTOS_LUNG_CANCER_UP	0.576	0.016	0.1658
1204	RADAEVA_RESPONSE_TO_IFNA1_DN	1.0987	0.016	0.1658
1674	DAVIES_MULTIPLE_MYELOMA_VS_MGUS_UP	0.9383	0.016	0.1658
1839	ZHAN_VARIABLE_EARLY_DIFFERENTIATION_GENES_UP	0.6857	0.016	0.1658
1981	HOSHIDA_LIVER_CANCER_SUBCLASS_S1	0.4358	0.016	0.1658
2457	KEGG_SULFUR_METABOLISM	0.9277	0.016	0.1658
2719	BIOCARTA_PLATELETAPP_PATHWAY	0.9778	0.016	0.1658
2928	REACTOME_GS_ALPHA_MEDIATED_EVENTS_IN_GLUCAGON_SIGNALING	0.584	0.016	0.1658
288	HUMMEL_BURKITTS_LYMPHOMA_DN	0.7217	0.018	0.1824
690	XU_HGF_TARGETS_INDUCED_BY_AKT1_48HR_UP	0.8726	0.018	0.1824
1295	HADDAD_T_LYMPHOCYTE_AND_NK_PROGENITOR_DN	0.585	0.018	0.1824
1324	REN_ALVEOLAR_RHABDOMYOSARCOMA_DN	0.3248	0.018	0.1824
1903	HOSHIDA_LIVER_CANCER_SURVIVAL_UP	0.5133	0.018	0.1824
2503	KEGG_AXON_GUIDANCE	0.2308	0.018	0.1824
3049	REACTOME_REGULATION_OF_INSULIN_SECRETION_BY_ACETYLCHOLINE	0.4752	0.018	0.1824
505	LUCAS_HNF4A_TARGETS_DN	1.1966	0.02	0.1989
1205	BECKER_TAMOXIFEN_RESISTANCE_DN	0.4479	0.02	0.1989
2119	RODWELL_AGING_KIDNEY_UP	0.3817	0.02	0.1989
2623	BIOCARTA_GCR_PATHWAY	0.5628	0.02	0.1989
2672	BIOCARTA_IL4_PATHWAY	0.8072	0.02	0.1989
3168	REACTOME_REGULATION_OF_INSULIN_SECRETION_BY_FREE_FATTY_ACIDS	0.484	0.02	0.1989

GSA was performed in R using the multiclass algorithm and the maxmean option. Gene sets from the C2 curated Molecular Signatures Database were considered for analysis. Enriched gene sets were chosen at a FDR of 0.2. Gene sets associated with EMT, metastasis, metaplastic breast carcinoma, or PI3K signaling are highlighted in bold.

Table S2. List of genes that are differentially expressed in *HER2*+*PIK3CA* tumors versus *HER2* tumors and *PIK3CA* tumors

Gene name	HER2+PIK3CA vs. HER2_diff	PIK3CA vs. HER2_diff	PIK3CA vs. HER2+ PIK3CA_diff	HER2+PIK3CA vs. HER2_p.val	PIK3CA vs. HER2_p.val	PIK3CA vs. HER2+ PIK3CA_p.val
Gm15429	1.606667	0.491667	−1.115	0.000323	0.320632	0.007682
LOC100041806	0.730476	0.185	−0.54548	4.88E-05	0.329382	0.000986
Amy2a4	1.391667	0.463333	−0.92833	0.000502	0.293938	0.013744
LOC100045516	0.284048	0.005	−0.27905	0.021735	0.998571	0.02417
Nlrp6	0.561429	−0.17333	−0.73476	0.02258	0.655528	0.003409
Mgat4b	0.880238	0.398333	−0.4819	0.000291	0.096373	0.032633
Nt5m	0.27119	0.018333	−0.25286	0.013219	0.975663	0.020647
Rdh14	−0.4369	−0.11	0.326905	0.005015	0.646751	0.033732
C030046I01Rik	0.53881	0.003333	−0.53548	0.019384	0.999817	0.020139
Rhoa	0.783333	0.085	−0.69833	4.48E-05	0.802684	0.000158
Capn1	0.671429	0.218333	−0.4531	0.00273	0.438416	0.039059
Cobl	1.311667	0.205	−1.10667	0.008218	0.860822	0.024873
Bcar1	0.48	0.06	−0.42	0.009123	0.91079	0.021854
Cryba1	1.327143	−0.04833	−1.37548	0.020149	0.993746	0.0161
Cyp2c40	1.733095	0.648333	−1.08476	0.001501	0.29476	0.040201
Cyp2d10	1.686667	0.173333	−1.51333	0.009805	0.93988	0.019968
Dbnl	0.559048	0.183333	−0.37571	0.002919	0.438162	0.041641
F2	1.482857	0.276667	−1.20619	0.008664	0.810905	0.031978
Fabp1	2.238571	0.738333	−1.50024	0.000594	0.311874	0.01494
Fga	1.23119	0.203333	−1.02786	0.014219	0.867021	0.041098
Flot2	0.268571	−0.19	−0.45857	0.040179	0.189835	0.000819
H19	1.665	0.503333	−1.16167	0.000146	0.277476	0.004123
Igf2	1.48381	0.563333	−0.92048	0.001164	0.266381	0.036227
Igfbp1	2.098571	0.863333	−1.23524	0.000502	0.165591	0.029553
Inppl1	2.162381	0.231667	−1.93071	0.000149	0.841454	0.000475
Itih3	1.48619	0.273333	−1.21286	0.010273	0.823479	0.035881
Klf1	0.587381	−0.125	−0.71238	0.002707	0.694209	0.000472
Kng1	2.130238	0.59	−1.54024	0.001907	0.517644	0.020707
Lect2	0.914048	0.205	−0.70905	0.009683	0.746881	0.044806
Lor	1.467143	0.598333	−0.86881	0.001298	0.22889	0.049114
Man2a1	1.413095	0.146667	−1.26643	0.004102	0.923247	0.009295
Mns1	−1.74548	−0.76167	0.98381	0.000846	0.163371	0.049761
Neu1	0.478333	0.031667	−0.44667	0.01384	0.976966	0.021343
Nfe2l1	0.554286	0.175	−0.37929	0.001328	0.401229	0.022532
Nnat	1.656667	0.441667	−1.215	0.003856	0.594726	0.031291
Ogdh	0.738571	0.205	−0.53357	3.97E-05	0.256553	0.001129
Pax1	1.343333	0.28	−1.06333	0.007432	0.761963	0.033044
Pck1	2.577619	1.05	−1.52762	0.001067	0.216416	0.043825
Inpp5k	0.524048	−0.145	−0.66905	0.011603	0.658406	0.00175
Ring1	0.337381	0.038333	−0.29905	0.016944	0.937724	0.034508
Surf4	0.432381	−0.08667	−0.51905	0.044855	0.867942	0.015647
Slc30a6	−0.37143	−0.03667	0.334762	0.016794	0.952442	0.031229
Nudt18	0.802381	0.275	−0.52738	0.000109	0.184408	0.005328
Taok1	0.57	0.255	−0.315	0.000555	0.128982	0.043909
Tlx2	0.52	0.045	−0.475	0.01227	0.959601	0.021855
Scgb1a1	1.789286	0.665	−1.12429	0.002236	0.330131	0.049857
Vdac1	0.753571	0.058333	−0.69524	0.002538	0.951144	0.004853
Smgc	1.098095	0.281667	−0.81643	0.000214	0.41443	0.003331
Tgif2	−0.96286	−0.05667	0.90619	0.0114	0.980669	0.016984
Fgl1	1.909524	0.531667	−1.37786	0.002517	0.535364	0.025473
Smcr7	0.88119	0.333333	−0.54786	0.000221	0.166878	0.012764
Hexdc	0.555476	0.048333	−0.50714	0.001399	0.93002	0.003045
Ccdc9	0.402857	0.048333	−0.35452	0.008091	0.914788	0.019032
Map3k5	0.46381	0.05	−0.41381	0.006034	0.925017	0.013492
Vps25	0.282143	−0.235	−0.51714	0.04028	0.109069	0.000416
Bag3	0.741429	0.378333	−0.3631	0.000141	0.040055	0.040917
Fbxw4	0.72619	0.141667	−0.58452	0.014143	0.819814	0.049314
Abi2	−0.73119	−0.11333	0.617857	0.003967	0.836579	0.01349
Ctdspl2	−0.51762	0.06	0.577619	0.002561	0.894392	0.000977
Trim67	0.769524	0.291667	−0.47786	0.001858	0.302254	0.047458
Cyp2d22	1.178095	0.101667	−1.07643	0.019463	0.96507	0.032985
Clptm1	0.328095	−0.00833	−0.33643	0.013154	0.996518	0.011108

Table S2. Cont.

Gene name	HER2$^+$PIK3CA vs. HER2_diff	PIK3CA vs. HER2_diff	PIK3CA vs. HER2$^+$ PIK3CA_diff	HER2$^+$PIK3CA vs. HER2_p.val	PIK3CA vs. HER2_p.val	PIK3CA vs. HER2$^+$ PIK3CA_p.val
Tssc4	0.602619	0.06	−0.54262	0.011068	0.945334	0.021744
Bin3	0.709048	0.156667	−0.55238	0.005191	0.715424	0.02758
Nkain4	1.221905	0.71	−0.5119	1.06E-05	0.003817	0.02774
Lrp10	0.500238	−0.02667	−0.5269	0.002381	0.976129	0.001521
1810030J14Rik	1.610714	0.461667	−1.14905	0.001633	0.483168	0.020161
9130011J15Rik	0.37	0.086667	−0.28333	0.006983	0.706484	0.037766
Rnf186	0.760952	0.068333	−0.69262	0.012687	0.956996	0.023007
Slc39a8	1.695952	0.128333	−1.56762	0.007958	0.964911	0.013695
Dynll2	0.761429	−0.07833	−0.83976	0.008997	0.938314	0.004336
1110006G14Rik	0.573571	0.15	−0.42357	0.001944	0.555841	0.018425
Nufip2	0.290952	−0.185	−0.47595	0.004828	0.086382	4.24E-05
Aspscr1	0.459286	0.065	−0.39429	0.009806	0.889447	0.026008
Ankle2	0.439286	−0.19333	−0.63262	0.039099	0.49974	0.003455
2310047M10Rik	0.868095	0.41	−0.4581	0.000165	0.063119	0.029486
Thoc3	0.676905	0.073333	−0.60357	0.017279	0.943536	0.033974
Rasgef1c	2.422857	1.06	−1.36286	5.87E-05	0.057899	0.010931
Shpk	0.809762	0.06	−0.74976	0.000815	0.94246	0.001638
Cpa5	0.57119	−0.17167	−0.74286	0.001273	0.431892	9.25E-05
Ddit4	1.358571	0.658333	−0.70024	0.000345	0.077597	0.048938
Wdr54	−0.51643	−0.01667	0.499762	0.016905	0.994802	0.020734
Gpsm2	−0.5869	0.076667	0.663571	0.021029	0.923851	0.009411
Ip6k2	0.293571	−0.03	−0.32357	0.001078	0.899628	0.000428
Dcst1	0.480714	−0.05333	−0.53405	0.010755	0.932093	0.004999
Mvp	0.82881	0.165	−0.66381	0.004048	0.747764	0.019321
Celf3	0.802857	0.27	−0.53286	0.002476	0.407214	0.040079
Wsb1	0.713333	0.208333	−0.505	0.000722	0.409268	0.011889
Cdk5rap3	0.477381	−0.18833	−0.66571	0.006195	0.376851	0.000335
Hamp	1.175952	0.513333	−0.66262	0.000133	0.081902	0.017648
Rnf123	0.42881	0.006667	−0.42214	0.002527	0.997973	0.002878
Tprn	0.81119	0.155	−0.65619	0.002216	0.733615	0.011229
Cog8	0.479286	−0.00333	−0.48262	0.006893	0.999685	0.006549
Sgsm2	0.766905	0.225	−0.5419	5.47E-07	0.063757	4.10E-05

Microarray data were analyzed by ANOVA using a three-class comparison and an FDR cutoff of 0.1. Genes that are differentially expressed ($P < 0.05$, Tukeys multiple comparison test) between both *HER2$^+$PIK3CA* vs. *HER2* tumors and *HER2$^+$PIK3CA* vs. *PIK3CA* tumors are shown.